

## Synthesis and Characterization of HPMpFBP Using Raman Spectroscopy, Nuclear Magnetic Resonance (NMR) Spectroscopy, and FTIR

Wilda Tri Putri Yusri<sup>1</sup>, Yulkifli Yulkifli<sup>1</sup>, Alizar Alizar<sup>2</sup>, Ilyas Md Isa<sup>3</sup>

<sup>1</sup> Department of Physics, Padang State University, Padang, Indonesia

<sup>2</sup> Department of Chemistry, Padang State University, Padang, Indonesia

<sup>3</sup> Department of Chemistry, Sultan Idris University of Education, Tanjung Malim, Malaysia

Article Info	ABSTRACT
<p><b>Article History:</b></p> <p>Accepted: May 24, 2021 Revised: July 19, 2021 Received: August 05, 2021</p> <hr/> <p><b>Keywords:</b></p> <p>FTIR HPMpFBP Nuclear Magnetic Resonance (NMR) Spectroscopy Raman Spectroscopy Synthesis</p> <hr/> <p><b>Corresponding Author:</b></p> <p>Ilyas Md Isa Email: <a href="mailto:ilyas@fsmt.upsi.edu.my">ilyas@fsmt.upsi.edu.my</a></p>	<p>Synthesis is one of the models for the formation of a new drug or compound with the aim of obtaining better activity at an economical price. HPMpFBP has been synthesized by mixing of 1-phenyl-3-methyl-5-pyrazolone and 4-fluorobenzoyl chloride. In the synthesis of HPMpFBP, a new compound namely 1-phenyl-3-methyl-4-(4-fluorobenzoyl)-5-pyrazolone has been obtained. The sample then characterized by non-invasive methods using Raman spectroscopy, Nuclear Magnetic Resonance (NMR) Spectroscopy and FTIR. Through this characterization process, wavelength information, chemical shift, and functional groups (chemical structure) of HPMpFBP samples were obtained. HPMpFBP has a chemical structure of C<sub>17</sub>H<sub>13</sub>N<sub>2</sub>O<sub>2</sub>F, the highest wavelength carried out by characterization using Raman is 1643.91 cm<sup>-1</sup>, the highest chemical shift characterized by using NMR (Nuclear Magnetic Resonance) is 7.8628 ppm, and the functional groups identified by using FTIR are (O-H, C-H, C=C, C=O, C-N). Information from the HPMpFBP sample characterization process using mentioned characterization methods was compared with previously reported results.</p> <p style="text-align: right;">Copyright © 2021 Author(s)</p>

### 1. INTRODUCTION

Creating a new compound requires modifying the chemical structure through chemical reactions in one way, namely synthesis. The synthesis is expected to form a new compound with a higher pharmacological activity than the parent compound (Purwanto, 2013). In the synthesis process, there is a reflux process where the reflux process aims to speed up the reaction by heating but will not reduce the number of substances present. Reflux is done to speed up the reaction by heating but not reduce the amount of substance present (Fatimura, 2017). In the synthesis process, there will be a reflux distillation process. Where reflux is a process that must be passed so that the reactions that occur can run more quickly and perfectly so that the results are obtained with a fairly good yield.

HPMpFBP is a compound obtained from a synthesis process carried out by mixing materials or substances used to obtain the results of the HPMpFBP synthesis compound. HPMpFBP is often referred to as 1-Phenyl-3-Methyl-4-(4-Fluorobenzoyl)-5-Pyrazolone (Jensen et al., 1959; Mustaffa & Ilyas Md Isa., 2011). Where the main ingredients of HPMpFBP synthesis are 1-Phenyl-3-Methyl-5-Pyrazolone and 4-Fluorobenzoyl chloride. The compound 1-phenyl-3-methyl-5-pyrazolone has a chemical structure

of  $C_{10}H_{10}N_2O$  with a molecular weight of 174.2, boiling point  $549^{\circ}F$  at 105 mm Hg, and melting point  $261^{\circ}-266^{\circ}F$ . Furthermore, 4-fluorobenzoyl chloride has a chemical structure of  $C_7H_4ClFO$  with a molecular weight of 158.56, boiling point 481.99 (K), a melting point 287.53 (K), and a density of 39.41 (Bar) at 682.73(K). Therefore, from the HPMpFBP synthesis process a chemical structure is obtained  $C_{17}H_{13}N_2O_2F$ . A picture of the chemical structure of HPMpFBP can be seen in Figure 1. The synthesis of HPMpFBP had been carried out by other researchers with the same and different compound names. Jensen et al. (1959), and Mustaffa & Illyas Md Isa (2011) named their synthesis result as HPMpFBP, while Meera et al. (2004) and Remya et al. (2006) named their synthesis result as HPMFBP. In this study, the authors followed the synthesis of Jensen et al. (1959), and Mustaffa & Illyas Md Isa (2011) but there are different ingredients and different amounts of the many substances used, the differences can be seen in Figure 2.

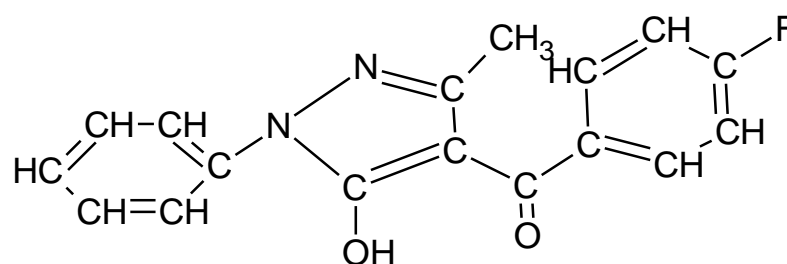


Figure 1. HPMpFBP chemical structure

In this study, the HPMpFBP compound was characterized using non-invasive techniques, namely by using Raman Spectroscopy, NMR (Nuclear Magnetic Resonance) and FTIR. The HPMpFBP had been synthesized by Jensen et al. (1959), and Mustaffa & Illyas Md Isa (2011) but the HPMpFBP samples had not been characterized so that how many functional groups were present in the samples is still unknown. Then Saleh et al. (1990), Meera et al. (2004), Remya et al. (2006), and Petrova et al. (2011) have also synthesized and characterized HPMpFBP samples using Nuclear Magnetic Resonance (NMR) Spectroscopy and FTIR. However, they did not use Raman Spectroscopy as a comparison between the main ingredient, namely PMP (1-phenyl-3-methyl-5-pyrazolone) and HPMpFBP after being added with other ingredients.

Raman bias is expressed in the form of friction energy from a given radiation ( $\Delta cm^{-1}$ ) but simplified to  $cm^{-1}$  (Holze, 2007). The NMR parameter is a chemical shift that is usually expressed in ppm from an internal reference and provides information on the type of hydrogen and carbon bound to each nucleus (Hore, 2015). Infrared spectra contain many absorption bands which are associated with the vibration system / vibration in the molecule. Each molecule has unique characteristics, so it is necessary to identify comparisons made under the same conditions (Sastrohamidjojo, 2001).

The characterization results obtained by Mustaffa & Illyas Md Isa (2011) are the infrared spectrum (IM) shows  $\nu(C-H)$ ,  $3060\text{ cm}^{-1}$ ;  $\nu(\text{stick } OH \cdots O)$ ,  $2600\text{ cm}^{-1}$ ;  $\nu(\text{pyrazolone bracelet stretch})$ ,  $1458\text{ cm}^{-1}$ ;  $\nu(C-O)$ ,  $1200\text{ cm}^{-1}$ ; and  $\nu(\text{bending from zero})$ , doublet line  $800\text{ cm}^{-1}$ . On the  $^1H$  NMR spectrum, the pepper displacement is 7.20-8.00 ppm. While, the characterization results obtained by Meera et al. (2004) and Remya et al. (2006) are  $^1H$  NMR ( $CDCl_3$ ) data :  $\delta$  (ppm) 7.17-7.87, and IR (KBr) data ( $\nu\text{ cm}^{-1}$ ); 2800, 1620 (C=O), 1590, 1500, 1356, 1214, 752; Elemental analysis: calculated for  $C_{17}H_{13}N_2O_2F$ . In the spectrum  $^1H$  NMR spectrum of HPMFBP, no peak corresponding to the enolic -OH has been observed. However, the absence of a peak at  $\delta$  3.4 ppm, corresponding to the methylene proton at the fourth position of the pyrazolone ring, confirms the existence HPMFBP in the enolic form.

Asnawati et al (2013) stated that the characterization of biosensors using  $FcGOxCP/GOx/CA$  material against glucose with a regression coefficient of 0.996 with a linear range of 0.1-3 mM; detection limit of 0.01 mM; sensitivity of  $0.989\text{ }\mu A / mM$ ; reproducibility of 0.07-0.3%; lifetime 1 day. Utamiyanti et al. (2016) stated that the material that can be used to detect glucose is  $SiO_2-CuO$  (B) material with the resulting sensitivity and detection limit values of  $0.7691\text{ }\mu A/mM$  and 0.1607 mM. Wahyuono et al. (2017) conducted a test to detect glucose levels in blood using the Raman method with the results of the Raman scattering at  $1121\text{ cm}^{-1}$  resulting in measurements with high linear correlation and good

sensitivity. Mohd Yazid et al.(2014) conducted a review of several glucose biosensor materials and found that zinc oxide and nickel oxide materials with high isoelectric point (IEP) can be used as an electrode material for glucose biosensors.

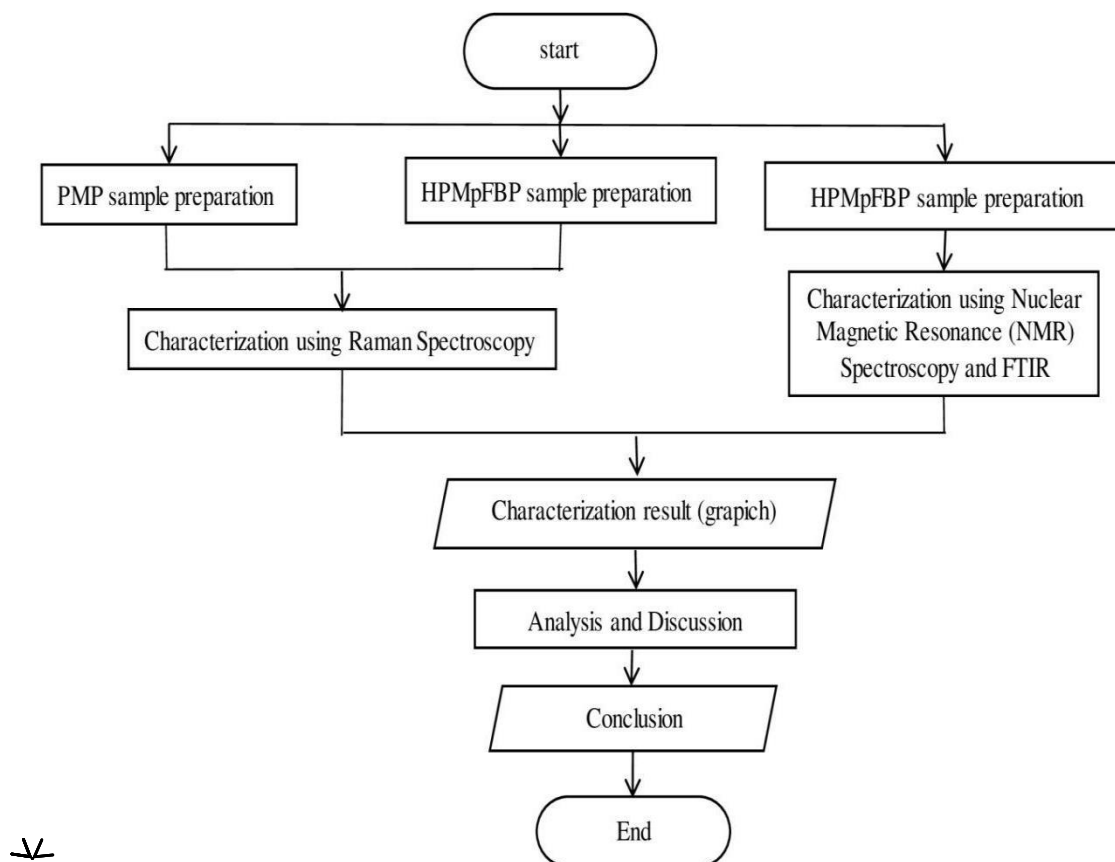


**Figure 2.** Steps of HPMpFBP characterization.

This study aims to synthesize and characterize the HPMpFBP samples used for glucose level detectors using a non-invasive method. The non-invasive methods used are Raman spectroscopy, Nuclear Magnetic Resonance (NMR) Spectroscopy and FTIR which will later provide information about wavelengths, chemical shifts and functional groups contained in the HPMpFBP sample. Furthermore, the results were compared with previous researches (Jensen et al., 1959; Meera & Reddy, 2004; Mustafa & Illyas Md Isa., 2011; Petrova et al., 2011; Remya et al., 2006; Saleh et al., 1990). Then, we perform an analysis of the HPMpFBP sample whether it can be used for glucose detectors or not.

## 2. METHOD

The stages of this research are sample preparation, the HPMpFBP synthesis process, HPMpFBP sample characterization using Raman Spectroscopy, Nuclear Magnetic Resonance (NMR) Spectroscopy, and FTIR (Figure 2). Jensen (1959), Mustafa & Illyas Md Isa (2011) and Petrova et al. (2011) had carried out a different synthesis method of HPMpFBP and a slightly different material than our work, but had almost the same chemical shift value. The amount of substances and materials used were also different. Furthermore, while  $\text{Ca}(\text{OH})_2$  normally used by other researchers, we used NaOH as the material. The research stages carried out for the synthesis of the HPMpFBP carried out in this study are depicted in the flow chart shown in Figure 3.

Data processing from the HPMpFBP characterization process used Origin software and the ACD/NMR Processor Academic Edition. Data characterization using Raman Spectroscopy was carried

out in two aspects, namely by comparing the results of the PMP sample characterization with HPMpFBP. The data obtained from the characterization process using Origin software are analyzed. This software will be generated data values in the function of wavelength and Raman shift. In characterizing HPMpFBP using Nuclear Magnetic Resonance (NMR) Spectroscopy, a graph of chemical shift and absorption will be generated. In the sample analysis process using Nuclear Magnetic Resonance (NMR) Spectroscopy, the ACD / NMR Processor Academic Edition software was used. The results were compared with previous studies (Meera & Reddy, 2004; Petrova et al., 2011; Remya et al., 2006; Saleh et al., 1990).

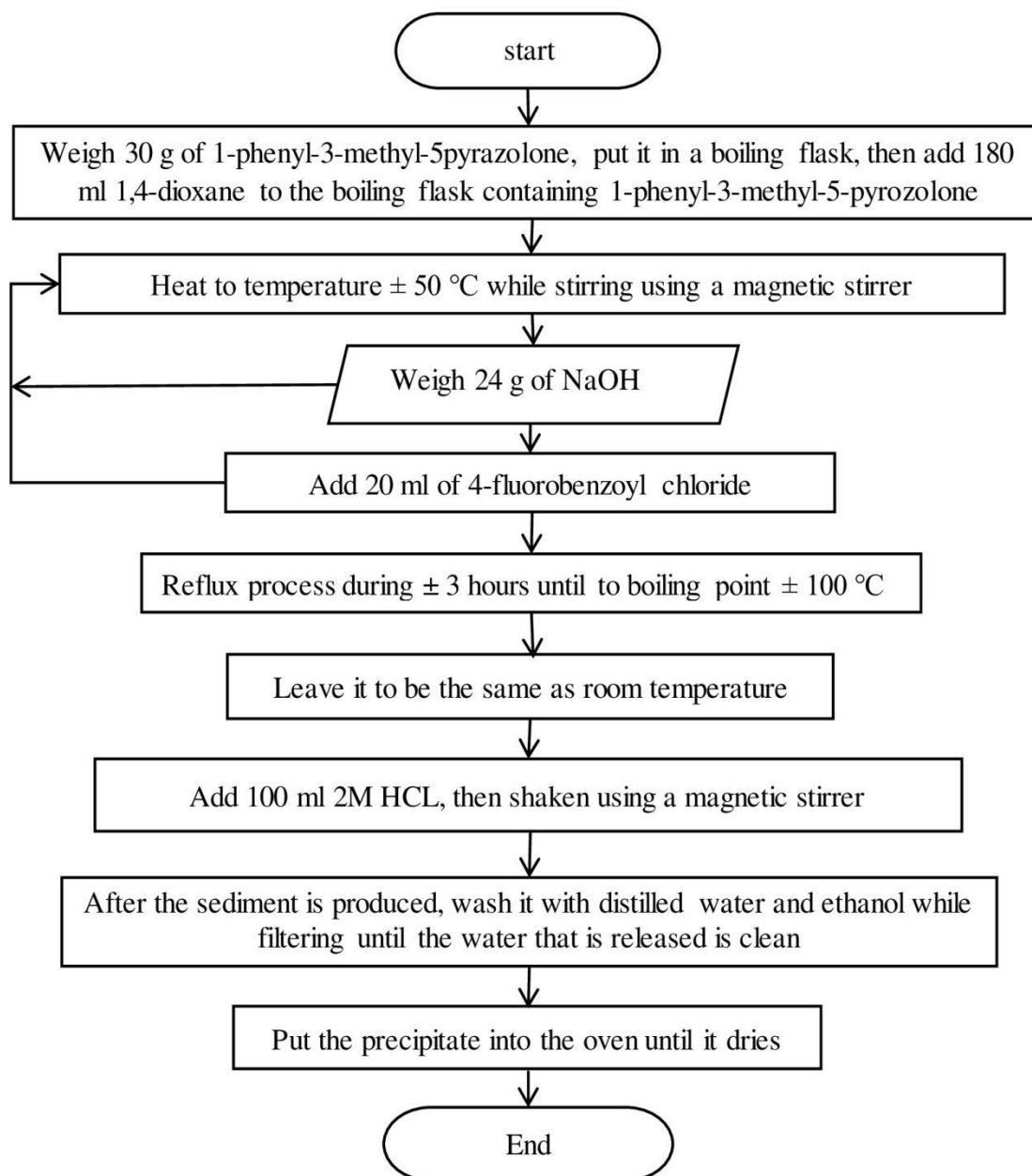


**Figure 3.** Steps of the HPMpFBP sample synthesis process.

Characterization using FTIR produce a graph in the form of wavelength, functional group and intensity of the energy function of sample. The Origin software was used to obtain the value of the wavelength of HPMpFBP sample and the result was compared with other studies (Meera & Reddy, 2004; Mustafa & Ilyas Md Isa., 2011; Remya et al., 2006).

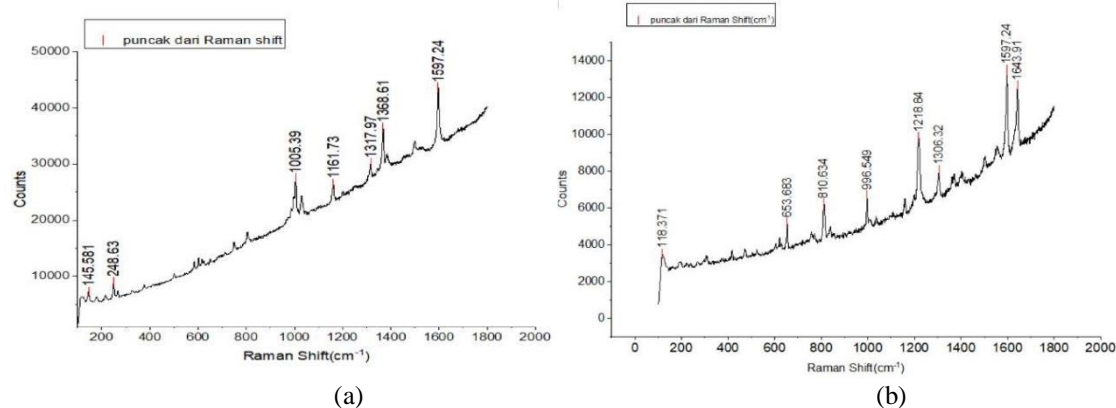


**Figure 4.** (a) The results of PMP and (b) HPMpFBP from characterization using Raman Spectroscopy.

### 3. RESULTS AND DISCUSSION

#### 3.1 Characterization of HPMpFBP Using Raman Spectroscopy

The results of the PMP and HPMpFBP analysis from characterization using Raman Spectroscopy can be seen in Figure 4. The peaks of the PMP data from Origin software were observed at 145.581  $\text{cm}^{-1}$ , 248.63  $\text{cm}^{-1}$ , 1005.39  $\text{cm}^{-1}$ , 1317.97  $\text{cm}^{-1}$ , 1368  $\text{cm}^{-1}$ , and 1597.24  $\text{cm}^{-1}$  (Figure 4a). The peaks of the HPMpFBP were observed at 118.371  $\text{cm}^{-1}$ , 653.683  $\text{cm}^{-1}$ , 810.634  $\text{cm}^{-1}$ , 996.549  $\text{cm}^{-1}$ , 1218.84  $\text{cm}^{-1}$ , 1306.32  $\text{cm}^{-1}$ , 1597.24  $\text{cm}^{-1}$ , and 1643.91  $\text{cm}^{-1}$  (Figure 4b). Thus, the highest wavelength is at 1643.91  $\text{cm}^{-1}$ . From Figure 4 (a) it can be seen the highest wavelength for PMP data is 1597.24  $\text{cm}^{-1}$ , while the highest wavelength for HPMpFBP 1643.91  $\text{cm}^{-1}$ . There is a wavelength difference of 46.67  $\text{cm}^{-1}$ . Table 1 summarizes the comparison between the results of PMP and HPMpFBP.

**Table 1.** Comparison of the results of PMP and HPMpFBP.

PMP characterization results	HPMpFBP characterization results
145.581 $\text{cm}^{-1}$	118.371 $\text{cm}^{-1}$
248.63 $\text{cm}^{-1}$	653.683 $\text{cm}^{-1}$
1005.39 $\text{cm}^{-1}$	810.634 $\text{cm}^{-1}$
1161.73 $\text{cm}^{-1}$	996.549 $\text{cm}^{-1}$
1317.97 $\text{cm}^{-1}$	1218.84 $\text{cm}^{-1}$
1368.61 $\text{cm}^{-1}$	1306.32 $\text{cm}^{-1}$
1597.24 $\text{cm}^{-1}$	1597.24 $\text{cm}^{-1}$
-	1643.91 $\text{cm}^{-1}$

#### 3.2 Characterization of HPMpFBP using Nuclear Magnetic Resonance (NMR) Spectroscopy

Figure 5 shows the results of HPMpFBP analysis using ACD / NMR Processor Academic Edition software. The results of NMR characterization can be seen in Table 2. We obtained the highest chemical shift of 7.8628 ppm. Other researchers (Meera & Reddy, 2004; Petrova et al., 2011; Remya et al., 2006; Saleh et al., 1990) obtained the highest chemical shift for HPMpFBP samples of 7.87 ppm. Thus, our result is similar to some previous studies.

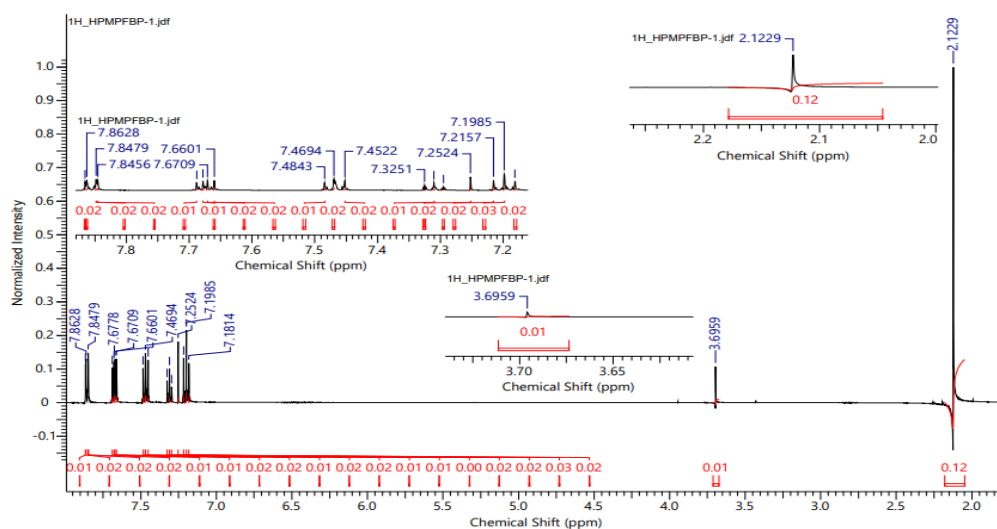


**Figure 5.** Results of HPMpFBP analysis using ACD / NMR Processor Academic Edition software.

**Table 2.** Comparison of the HPMpFBP from current study with Saleh et al. (1990).

Chemical Shift (ppm)	Current study	Saleh et al. (1990)	Functionl Group in the $^1\text{H}$ NMR
7.8-7.9 (ppm)	7.8456 ppm	7.852 ppm	$\text{CH}_3\text{-N} \begin{array}{l} \diagdown \\ \diagup \end{array}$ $\text{CH}_3\text{-C=O}$
	7.8479 ppm	7.856 ppm	
	7.8628 ppm	7.867 ppm	
		7.870 ppm	
7.6-7.7 (ppm)	7.6601 ppm	7.662 ppm	$\text{CH}_3\text{-N} \begin{array}{l} \diagdown \\ \diagup \end{array}$ $\text{CH}_3\text{-C=O}$
	7.6709 ppm	7.671 ppm	
		7.682 ppm	
		7.691 ppm	
		7.695 ppm	
7.4-7.5 (ppm)	7.4522 ppm	7.456 ppm	$\text{CH}_3\text{-C=O}$
	7.4694 ppm	7.462 ppm	
	7.4843 ppm	7.472 ppm	
7.3-7.4 (ppm)	7.3251 ppm	7.300 ppm	$\text{H-C} \equiv$
		7.314 ppm	
		7.325 ppm	
		7.328 ppm	
		7.382 ppm	
7.1-7.26 (ppm)	7.1985 ppm	7.183 ppm	$\text{H-C} \equiv$
	7.2157 ppm	7.191 ppm	
	7.2524 ppm	7.199 ppm	
		7.205 ppm	
		7.213 ppm	
		7.221 ppm	
		7.261 ppm	

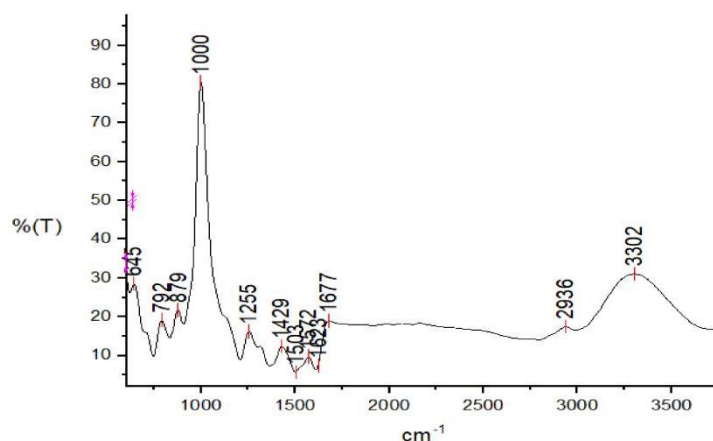


Figure 6. Results of HPMpFBP analysis using Origin software.

### 3.3 Characterization of HPMpFBP Using FTIR

The results of the HPMpFBP analysis using Origin software can be seen in Figure 6 and wavelength and functional groups resulting from the analysis process is given in Table 3. The results were compared with that obtained by Meera et al. (2004) and Remya et al. (2006). Our result is slightly different from Meera et al. (2004) and Remya et al. (2006). In the O-H functional group, we obtained a wavelength value of 3302  $\text{cm}^{-1}$ , while Meera et al. (2004), Remya et al. (2006) obtained a wavelength value of 2800  $\text{cm}^{-1}$ , but for the functional group from the infrared table there is no wavelength range value obtained. The area between 2000-4000  $\text{cm}^{-1}$  is a special area which is often very complicated, because the vibration of stretches and bends causes absorption in this area (Lau, 2011).

**Table 3.** Comparison of the HPMpFBP analysis from current study with Meera et al. (2004) and Remya et al. (2006).

Current study		Meera et al. (2004)		Remya et al. (2006)	
Wavelength	Functional groups	Wavelength	Functional groups	Wavelength	Functional groups
3302 $\text{cm}^{-1}$	O-H	-	-	-	-
2936 $\text{cm}^{-1}$	C-H	1356 $\text{cm}^{-1}$	C-H	1356 $\text{cm}^{-1}$	C-H
1429 $\text{cm}^{-1}$	C-H				
879 $\text{cm}^{-1}$	C-H	752 $\text{cm}^{-1}$	C-H	752 $\text{cm}^{-1}$	C-H
792 $\text{cm}^{-1}$	C-H				
1623 $\text{cm}^{-1}$	C=O	1620 $\text{cm}^{-1}$	C=O	1620 $\text{cm}^{-1}$	C=O
1572 $\text{cm}^{-1}$	C=C	1590 $\text{cm}^{-1}$	C=C	1590 $\text{cm}^{-1}$	C=C
1503 $\text{cm}^{-1}$	C=C	1500 $\text{cm}^{-1}$	C=C	1500 $\text{cm}^{-1}$	C=C
1255 $\text{cm}^{-1}$	C-N	1214 $\text{cm}^{-1}$	C-N	1214 $\text{cm}^{-1}$	C-N

In the C-H functional group, we obtained a wavelength value of 792-2936  $\text{cm}^{-1}$  while Meera et al. (2004) and Remya et al. (2006) obtained a wavelength value of 752-1356  $\text{cm}^{-1}$ . There is a shift from the three results which may be due to the overlap of the strain absorbance of the bonds which cause difficulties in analysis (Dachriyanus, 2004).

A wavelength value of 1623  $\text{cm}^{-1}$  was obtained for the C=O functional group. This value is close 1620  $\text{cm}^{-1}$  from Meera et al. (2004) and Remya et al. (2006). Thus, there is a shift of 3  $\text{cm}^{-1}$ . The position of the absorption band can vary depending on the type of compound and its environment (Dachriyanus, 2004). In the functional group C=C, we obtained a wavelength value of 1503-1572  $\text{cm}^{-1}$ , while Meera et al. (2004) and Remya et al. (2006) obtained a wavelength value of 1500-1590  $\text{cm}^{-1}$ . At these

wavelengths, there are differences in the structure and arrangement of the molecules that cause the distribution of the absorption peak to change due to various interactions so that they cannot be interpreted correctly.

In the C-N functional group, the authors obtained a wavelength value of  $1255\text{ cm}^{-1}$  while Meera et al. (2004) and Remya et al. (2006) obtained a wavelength value of  $1214\text{ cm}^{-1}$ . At this wavelength value there is also a difference of  $41\text{ cm}^{-1}$ , this is because at a wavelength of  $500\text{-}1500\text{ cm}^{-1}$  it has a very complicated absorption where there will be an overlap of the CX bond strain absorbance (X=O, N, S, P and halogens) which will cause difficulties in the analysis (Dachriyanus, 2004).

#### 4. CONCLUSION

This research has succeeded in producing the compound HPMpFBP from the synthesis process mixing between 1-phenyl-3-methyl-5-pyrazolone + NaOH + 4-fluorobenzoyl chloride + HCL. The compound was named by 1-phenyl-3-methyl-4-(4-fluorobenzoyl)-5-pyrazolone or abbreviated as HPMpFBP. The HPMpFBP has a chemical structure of  $\text{C}_{17}\text{H}_{13}\text{N}_2\text{O}_2\text{F}$  with the highest wavelength of Raman Spectroscopy characterization of  $1643.91\text{ cm}^{-1}$ . The chemical shift from Nuclear Magnetic Resonance (NMR) Spectroscopy characterization is less than 8 ppm. Finally, a functional groups from characterization using FTIR is (O-H, C-H, C=O, C=C, C-N).

#### ACKNOWLEDGEMENT

This study was financially supported by the Grant Universitas Negeri Padang for the PTPT-PENELITIAN KERJASAMA PERGURUAN TINGGI LUAR NEGERI TERAPAN, No. Contract: 13/LT/2021.

#### REFERENCE

- Asnawati, A., Indarti, D., & Mulyono, T. (2013). Amperometric biosensor for glucose detection based-on immobilisation of glucose oxidase in acetic cellulose membrane using ferrocene as mediator. *Jurnal Ilmu Dasar*, 14(1), 45–51.
- Dachriyanus, P. D. (2004). *Structural Analysis of Organic Compounds by Spectroscopy*. LPTIK Andalas University.
- Fatimura, M. (2017). Tinjauan Teoritis Faktor-Faktor Yang Mempengaruhi Operasi Pada Kolom Destilasi. *Jurnal Media Teknik*, 11(1).
- Holze, R. (2007). E. Smith and G. Dent (eds): Modern Raman spectroscopy—a practical approach, Wiley, Chichester, United Kingdom, 2005, 210 + XI p., 24.95 £; ISBN 0471497940. *Journal of Solid State Electrochemistry*, 11(4). <https://doi.org/10.1007/s10008-005-0062-2>
- Hore, P. J. (2015). *Nuclear magnetic resonance*. Oxford University Press, USA.
- Jensen, B. S., Meier, H., Lundquist, K., & Refn, S. (1959). The Synthesis of 1-Phenyl-3-methyl-4-acyl-pyrazolones-5. *Acta Chemica Scandinavica*, 13. <https://doi.org/10.3891/acta.chem.scand.13-1668>
- Lau, W. S. (2011). Infrared Characterization for Microelectronics. In *Infrared Characterization for Microelectronics*. <https://doi.org/10.1142/9789812817464>
- Meera, R., & Reddy, M. L. P. (2004). Para-substituted 1-phenyl-3-methyl-4-acyl-5-pyrazolones as chelating agents for the synergistic extraction of thorium(IV) and uranium(VI) in the presence of various crown ethers. *Solvent Extraction and Ion Exchange*, 22(5). <https://doi.org/10.1081/SEI-200030290>
- Mohd Yazid, S. N. A., Md Isa, I., Abu Bakar, S., Hashim, N., & Ab Ghani, S. (2014). A review of glucose biosensors based on graphene/metal oxide nanomaterials. *Analytical Letters*, 47(11), 1821–1834.
- Mustaffa, A., & Ilyas Md Isa., M. I. S. (2011). Determination of Stability of Lanthanide Complexes La(III), Pr(III), Eu(III), Ga(III), Er(III), and Lu(III) with Fluorine 1-phenyl-3- methyl-4-benzoyl-

- 5-pyrazolone (HPMBP) using imaging methods. *J. Sains Dan Matematik*, 3(2), 1–10.
- Petrova, M. A., Kurteva, V. B., & Lubenov, L. A. (2011). Synergistic effect in the solvent extraction and separation of lanthanoids by 4-(4-fluorobenzoyl)-3-methyl-1-phenyl-pyrazol-5-one in the presence of monofunctional neutral organophosphorus extractants. *Industrial & Engineering Chemistry Research*, 50(21), 12170–12176.
- Purwanto, B. T. (2013). Modifikasi Struktur N-Fenilurea Menjadi Senyawa Baru N-Benzoilfenilurea dan 4-Fluorobenzoilfenilurea Serta Uji Aktivasnya sebagai Penekan Susunan Saraf Pusat. *Majalah Berkala Ilmiah Kimia Farmasi, Departemen Kimia Farmasi FF Unair*, 2(1), 28–32.
- Remya, P. N., Ambili Raj, D. B., & Reddy, M. L. P. (2006). Para-substituted 1-phenyl-3-methyl-4-aryol-5-pyrazolones as selective extractants for vanadium(V) from acidic chloride solutions. *Solvent Extraction and Ion Exchange*, 24(6). <https://doi.org/10.1080/07366290600952576>
- Saleh, M. I., Ahmad, M., & Darus, H. (1990). Solvent extraction of lanthanum (III), europium (III) and lutetium (III) with fluorinated 1-phenyl-3-methyl-4-benzoyl-5-pyrazolones into chloroform. *Talanta*, 37(7), 757–759.
- Sastrohamidjojo, H. (2001). Spectroscopy. *Yogyakarta: Liberty Yogyakarta*.
- Utamiyanti, I. F., Rumhayati, B., & Mulyasuryani, A. (2016). THE DEVELOPMENT OF GLUCOSE SENSOR BASED ON SiO<sub>2</sub>-CuO MATERIALS USING SCREEN PRINTED CARBON ELECTRODE (SPCE). *ALCHEMY Jurnal Penelitian Kimia*, 12(1), 50–60.
- Wahyuono, R. A., Roekmono, R., Hadi, H., Yuwono, R. A., & Muhimmah, L. C. (2017). Deteksi Kadar Glukosa Dalam Plasma Darah Terpisah Oleh Mikrofluida Terintegrasi Partikel Nano ZnO Berbasis Spektroskopi Inframerah Dan Raman. *Jurnal Integrasi Proses*, 6(4), 148–154.